Magnetic Resonance Imaging 61 (2019) 143–148

Contents lists available at ScienceDirect

Magnetic Resonance Imaging

journal homepage: www.elsevier.com/locate/mri

Case report

Mapping cerebral perfusion from time-resolved contrast-enhanced MR angiographic data

Muhammad Asaduddin[a], Won-Joon Do[a], Eung Yeop Kim[b,*], Sung-Hong Park[a,**]

[a] Department of Bio and Brain Engineering, Korea Advanced Institute of Science and Technology, Daejeon, South Korea
[b] Department of Radiology, Gil Medical Center, Gachon University College of Medicine, Incheon, South Korea

A B S T R A C T

A common method to acquire both perfusion and angiographic information is to have separate MRI scans for each information. In this study, we propose to achieve the goal by deriving perfusion parameters, specifically cerebral blood volume (CBV) and Tmax, from time-resolved contrast-enhanced magnetic resonance angiography (CE-MRA). Both CE-MRA and DSC-MRI were performed on seven subjects with a diagnosed ischemic stroke. Concentration functions from CE-MRA were modeled using a modified gamma-variate function to appreciate the full first-pass transition of the tracer bolus. Perfusion parameters were calculated using concentration function derived from each imaging method and were compared to each other both visually and quantitatively by means of correlation studies. CBV and Tmax maps generally showed good agreement between the two methods. This study proved the concept of using time-resolved CE-MRA as both vascular imaging and tissue perfusion mapping while using a single injection of contrast agent, potentially reducing cost and improving patient safety and comfort.

1. Introduction

Dynamic susceptibility contrast (DSC) and time-resolved contrast-enhanced MR angiography (CE-MRA) are routine protocols for clinical diagnosis of cerebrovascular diseases. Both techniques share some common aspects (e.g. injection of contrast agent), but provide different clinical information. DSC is commonly used for evaluation of perfusion parameters including cerebral blood volume (CBV) and time-to-maximum (Tmax). Typically hemodynamic characteristics are altered in and around a lesion of specific brain area, which is reflected in perfusion parameters and shown as hyper- or hypo-perfusion in most cases [1,2]. Mapping of these parameters provides physicians with more accurate diagnostic information on the areas impacted by the lesion. An early stage of brain diseases may not be discovered with conventional anatomical imaging, but often detectable with perfusion parameters such as Tmax and MTT. In case of stroke, such indicators have been widely used for assessment of salvageable tissue. Reperfusion treatment is performed to tissues where the damage is indicated in perfusion maps but not seen in diffusion-weighted imaging (DWI). Although reliability of such mismatch analysis remains controversial, it has been widely used as early indicators of revascularization therapy [3,4].

Time-resolved contrast-enhanced MR Angiography (CE MRA) is performed by repeated vascular imaging with bolus injection of contrast agent. It is used to evaluate vascular structure and blood dynamics within the vessels, which are the main criteria to determine the revascularization therapy in case of ischemic stroke. CE-MRA images are derived through subtraction between T1-weighted images with and without contrast agent. The dynamic acquisition of T1-weighted images for CE-MRA is similar to that for dynamic contrast enhanced (DCE) MRI in that both scans require injection of contrast agent [5,6]. Therefore, a model from DCE perfusion assessment may be used to evaluate concentration function of CE-MRA data, which has not been explored well so far.

Acquiring both DSC and CE-MRA data would provide an all-encompassing view on the hemodynamics of a patient. However, both scans use gadolinium-based contrast agent potentially harmful to patients with kidney dysfunction because of higher chances of promoting diseases such as Gd deposition in the brain or nephrogenic systemic fibrosis (NSF). It also takes a long scanning time to apply both techniques. A new technique that resolves these problems will improve safety and save cost for the patients.

This research aims to utilize and manipulate dynamic MR Angiography data to additionally produce perfusion maps (CBV and Tmax). We adopted and modified the DCE model and the DSC model for processing the CE-MRA data. This research will contribute to decreasing the amount of contrast agent or providing additional information with the same amount of contrast agent compared to the conventional method.

* Correspondence to: E. Y. Kim, Department of Radiology, Gil Medical Center, Gachon University College of Medicine, 21, Namdong-daero 774 beon-gil, Namdong-gu, Incheon 21565, South Korea.
** Correspondence to: S.-H. Park, Department of Bio and Brain Engineering, Korea Advanced Institute of Science and Technology, Rm 1002, CMS (E16) Building, 291 Daehak-ro, Yuseong-gu, Daejeon 34141, South Korea.
E-mail addresses: neurorad@gachon.ac.kr (E.Y. Kim), sunghongpark@kaist.ac.kr (S.-H. Park).

https://doi.org/10.1016/j.mri.2019.05.040
Received 31 January 2019; Received in revised form 24 May 2019; Accepted 27 May 2019

2. Materials and methods

2.1. Theory

DSC-MRI measures the dynamic T2* or T2 signal reduction during the first pass of paramagnetic intravascular contrast through the cerebrovascular system. Tracer concentration function (Cm(t)) is defined as the total concentration of tracer remaining in the voxel at a given time [2,7]. Signal intensity holds a relation with concentration function as described in the following Eq. (1), where reduction in image intensity is converted into higher concentration of contrast agent. Cerebral blood volume (CBV) is a measure of total blood volume transferred into a voxel during a bolus transit, useful for diagnosis of diseases such as hemorrhage or lack of neuron due to nutrient starvation. CBV is derived from concentration function of brain tissue and the feeding artery specified by the following Eq. (2) [2,8]:

$$C_m(t) = -\frac{k}{TE}\ln\left(\frac{S(t)}{S_0}\right) \tag{1}$$

$$CBV = k\frac{\int_{-\infty}^{\infty} C_t(t)}{\int_{-\infty}^{\infty} C_a(t)} \tag{2}$$

where $C_t(t)$ and $C_a(t)$ are tracer concentration functions from tissue and artery, respectively. Correction factor k is introduced to take into account tissue density, hematocrit differences, and feeding capillary size. For this research we set tissue density for all patients to be 1.04 g/ml [9] [10]. Hematocrit levels for small and large vessels were set at 0.42 and 0.32, respectively [7] [10]. Feeding artery and capillary diameters were set to be 30 μm and 8 μm, respectively [6,7,10,11].

Time-to-maximum (Tmax) is defined as an interval between the time of the first arrival of tracer bolus and the time of the tracer concentration function to reach its maximum in a voxel. It is known that Tmax for a specific tissue does not vary significantly (typically < 4 s), unless hemodynamic abnormality exists [12].

In this study we suggest to derive concentration function from time-resolved CE-MRA data. Zhang et al. (2012) [6] suggested the use of dye-dilution theory to create gamma-variate model, which represents bolus transition in voxel of interest. This theory suggests two different hemodynamic processes: a bolus influx without outflow, which is present in the early phase, and bolus influx with venous outflow in the later phase. These two processes are represented in the two separate equations as follows:

$$\begin{cases} C(t) = \dfrac{A}{1 + e^{-K_a(t-at-t_a)}} & t < t_b \\ C(t) = \dfrac{A}{1 + e^{-K_a(t-at-t_a)}} e^{-K_b(t-t_b)} & t \geq t_b \end{cases} \tag{3}$$

where each variable is correlated to a tracer kinetic property. A is equivalent to the maximum concentration in a voxel, K_a and K_b represents a constant of inflow and outflow while t_a and t_b is the arrival time and exit time of the tracer, respectively [6]. From this model, the full first-pass of the tracer bolus can be appreciated. The concentration functions from different voxel would be similar to each other in terms of shape with differences only in the magnitude and bolus arrival time. In this study the location for arterial input function was fixed in Sylvian segment of middle cerebral artery (MCA) throughout the whole analysis [13].

Concentration function has a well-defined relation with longitudinal relaxation R1 as shown in the following Eq. (4). The measured MR signal is affected by R1 as described in Eq. (5).

$$C_m(t) = \frac{R_1(t) - R_1(0)}{r1} \tag{4}$$

$$\frac{S(t)}{S_0} = \frac{1 - e^{-TR*R_1(t)}}{1 - e^{-TR*R_1(0)}} * \frac{1 - \cos(a)e^{-TR*R_1(0)}}{1 - \cos(a)e^{-TR*R_1(t)}} \tag{5}$$

Table 1
Occlusion site information for the patients.

Patient number	Occlusion site
1	Right distal internal carotid artery
2	Left M1 segment
3	Right M1 segment
4	Left M1 segment
5	Right proximal internal carotid artery
6	Right proximal internal carotid artery
7	Right M1 segment

After acquiring the concentration function, the same method was used to calculate CBV and Tmax values as the case of DSC mentioned above.

2.2. Data information

The study was performed for 7 stroke patients whose occlusion site information is described in Table 1. DSC and time-resolved CE-MRA data were sequentially acquired with two separate injections of contrast agent per each subject. DSC data was acquired in 2D echo planar imaging (EPI) with following parameters: time to repeat (TR)/echo time (TE) = 1751 ms/30 ms, matrix size = 128 × 128, field of view = 230 × 230 mm^2, slice thickness = 4 mm, number of slices = 20, and number of dynamic scans = 50. CE-MRA data was acquired in 3D Time-resolved angiography with stochastic trajectories (TWIST) with following parameters: TR/TE = 2.62 ms/0.95 ms, matrix size = 140 × 150 × 144, field of view = 300 × 400 × 172.8 mm^3, and number of dynamic scans = 33. DSC data were acquired in the axial direction while CE-MRA data were acquired in the coronal direction right after DSC with no waiting time. GADOVIST was injected for DSC and CE-MRA at a rate of 3 ml/s and 1.5 ml/s, respectively. Total amount of injection was 0.1 ml per kg of subject body weight. T1 of tissue and r1 of GADOVIST were assumed to be 1800 ms [14] and 5 s^{-1} mM^{-1} [15], respectively.

2.3. CBV and Tmax calculations

CBV and Tmax maps were derived from DSC and CE-MRA data as described in the theory section. Tissue concentration function Ct(t) used in CBV was calculated from each voxel within the imaging field of view. Singular value decomposition was used to minimize effects of temporal fluctuations due to noises for both DSC and CE-MRA. For arterial concentration function Ca(t), we chose the middle cerebral artery for its large enough size and proximity to the edge of the hemispheres. In this study, temporal resolution of DSC was greater than that of CE-MRA. This caused error in estimation for CE-MRA derived Tmax. In order to minimize the error, we estimated the time points of the peak and the bolus arrival by partially modeling signal. For a given Cm(t), we generated a line from the peak point to the signal point corresponding to 110% of the baseline concentration. Arrival time was then estimated as the intercept between the generated line and the time axis. This method was chosen for its higher reproducibility and better perfusion parameter estimation than existing methods such as modeling of the whole signal or assumption of no tracer delay (i.e., assumption of baseline Cm (t) = 0) [16]. In our procedure, we used a threshold of 110% of the baseline concentration, which was determined empirically and was consistent with the value from the previous literature [16]. Bolus exit time was estimated in a similar way to the bolus arrival time: (i) defining the line between the peak point and the signal point corresponding to 110% of the baseline concentration defined at the end after the bolus passage, (ii) finding the intercept between the generated line and the time axis. After estimating the bolus arrival time and the bolus exit time, CBV and Tmax were calculated from the bolus arrival time to the bolus exit time.

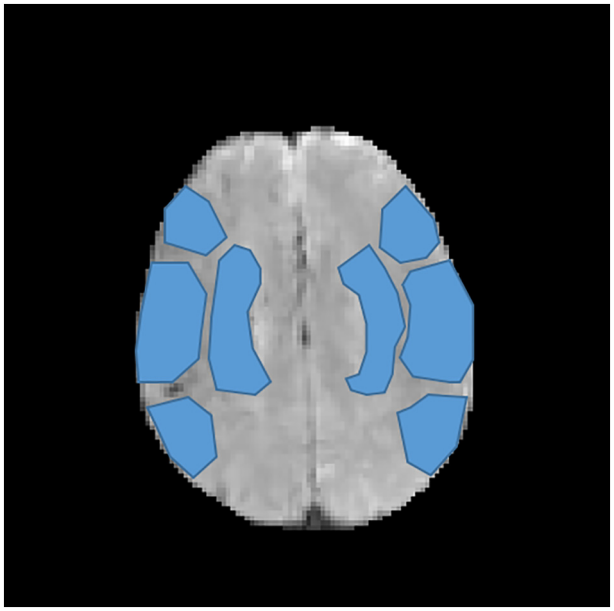

Fig. 1. Regions of interest (ROIs) for quantitative analyses. Three gray matter and one white matter ROIs were chosen in each hemisphere on 5 slices to generate 40 data pairs per subject with no discernible artefacts and/or pixel mismatch from non-rigid registration.

2.4. Comparison of DSC and DCE MRA

An intensity based multimodal image registration [17] was performed as available in MATLAB image processing toolbox based on the implementation of D. Mattes et al. [18]. Baseline images (before tracer arrival) and other supplemental information such as pixel dimensions from DSC and CE-MRA were fed into the registration algorithm. The optimizer and metrics were adjusted for the multimodal registration, under the assumption that DSC and CE-MRA data were from two different modalities.

Quantitative comparison was performed using structural similarity (SSIM), pixel-wise correlation, and ROI-based correlation. ROIs were determined by selecting 4 areas from each hemisphere while accounting for possible EPI distortion. Since EPI distortion mostly affects the frontal and occipital lobe, ROIs were located mostly in temporal lobe, basal nuclei, insular lobe, and diencephalon structures. The gray matter temporal area was split into three ROIs while white matter/basal ganglia were considered as one ROI. Total ROIs from a slice were 8 as exemplified in Fig. 1 and total five slices were taken from each patient. Correlation between the 40 data pairs was estimated to investigate the agreement between perfusion maps from DSC and CE-MRA. Linear regression was performed to find a trend that indicated the correlation. Correlation coefficients of pixel-wise and ROI-based data pairs were calculated between DSC and CE-MRA for both CBV and Tmax parameters.

3. Results

Concentration function Cm(t) curve from DSC showed normal bolus entry and exit. However, Cm(t) curve of CE-MRA showed remaining contrast agent even long after bolus transit, presumably due to the fact that for the T1-weighted imaging the signal recovery to the baseline takes longer after passage of the contrast agent. Therefore, the recovery portion of the Cm(t) from CE-MRA was estimated to calculate CBV in the same way as DSC.

Figs. 2 and 3 show representative CBV and Tmax maps from CE-MRA and DSC. Visual comparison suggested a good correlation between perfusion maps from CE-MRA and DSC. Gray matter and white matter perfusion signals were high and low, respectively, in both scans, as expected. These trends were well maintained in the lesion areas as well. DSC-derived Tmax maps often showed high signals in the boundary, presumably due to distortion effects of the EPI scan (Figs. 2b and 3b).

Correlation coefficients between DSC and CE-MRA are summarized in Table 2 and the ROI-based correlation plot is shown in Fig. 4. Correlation between the two methods was significant ($P < 0.05$), with relatively higher correlation coefficients for CBV than Tmax ($N = 7$). Upon checking the goodness of fit in Fig. 4, it was indicated that CBV maintained the trend more tightly than Tmax. CBV showed no significant difference between gray matter and white matter ROIs and between normal and pathologic ROIs, whereas Tmax showed significant differences for both of the ROI comparisons (Table 2). The pixel-wise correlation was lower than the ROI-based correlation, although still statistically significant ($p < 0.05$). Difference between ROI-based and pixel-wise comparisons is likely due to geometrical distortion of the EPI scan used for DSC, which may mismatch the location of hemodynamic activity. Despite the imperfectness of the method, variations in correlation between different patients were small in both parameters. This indicates the robustness of our method against various conditions of the patient.

Fig. 5 shows images from another representative patient, different from those in Figs. 2 and 3, demonstrating localization of the occlusion site in CBV and Tmax maps. In Fig. 5, left M1 occlusion can be seen readily in the Tmax map as indicated by the brown arrows, where Tmax was measured to be above 6 s. This abnormality is further demonstrated in the CBV maps in the form of blood volume reduction (hypo-perfusion) in reference to the contralateral normal side as indicated by white arrows.

4. Discussion

Delivery of nutrient and oxygen to the cerebral tissue is performed through microvasculature. Normal microvasculature contributes to 1–3% of the total volume of normal cerebral tissue. However, in the event of tumor or stroke, the vasculature will be greatly compromised due to rapid cell growth, increase in cell density, or interstitial pressure changes which will suppress vessels of the surrounding area [19,20]. Perfusion parameters detect changes in blood supply to cerebral cells far before any anatomical alteration takes place [21,22]. This advantage is useful for early detection and prevention of tumor or stroke. While there are some studies to compare DSC and DCE perfusion MRI [23,24], this study is the first to compare perfusion maps from DSC MRI and time-resolved CE MRA.

Compromised vasculature can also be detected from its anatomy using MR angiographic data. MR angiography can be done quickly with short post-processing. Anatomy and perfusion information is useful for indicating salvageable tissue [25,26]. However, acquiring anatomy and perfusion information from both DSC and CE-MRA requires a longer scan time and has a safety problem. Using gadolinium contrast agent twice may increase the risk of Gd deposition in the brain. Although techniques for minimizing Gd deposition are developed, it will take time for them to be used for real clinical practice.

The proposed method enables us to acquire perfusion map from MR angiography alone. This solves all the three limitations explained beforehand. Furthermore, the acquired perfusion map showed strong correlation to that of DSC which was acquired separately as control. Small degree of variations among patient (standard deviation of ± 0.10 and ± 0.11 for CBV and Tmax respectively) implied robustness of the proposed method.

The concentration function used in our experiment was extrapolated based on the dye-dilution theory [6]. Although this model is less sensitive to tracer delay, the calculation of CBV is dependent on the area under the curve of arterial input function. Therefore, there is possibility that the fitting of concentration function to this model may induce errors in CBV mapping. However, fitting was still preferable to get the

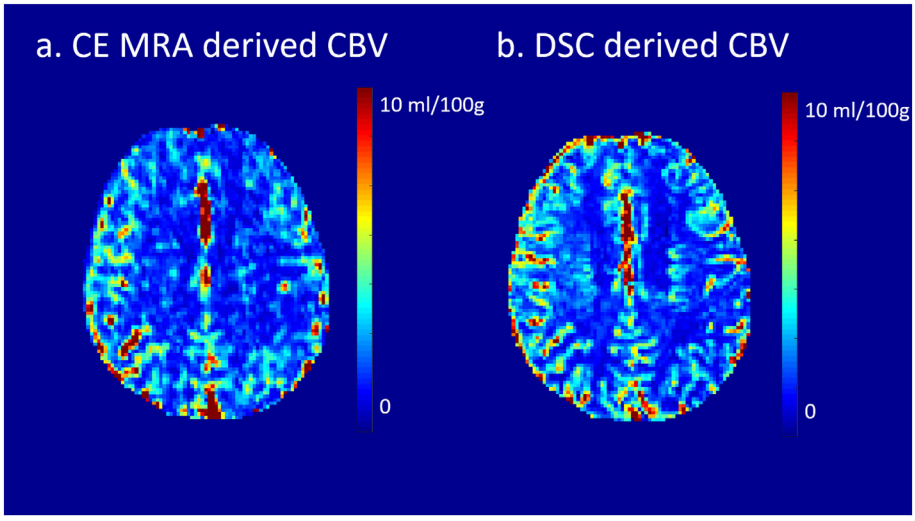

Fig. 2. Representative cerebral blood volume (CBV) maps from time-resolved contrast enhanced MR angiography (CE MRA) (a) and dynamic susceptibility contrast MRI (DSC) (b). Color scale bars represent the CBV values.

Tmax values consistent with those from literature [12,27]. Another issue in arterial input function is that it is unstable when occlusion exists around the area. Even with the occlusion existing outside the MCA ROI, the arterial input signal may undergo mild delay or dispersion due to the occlusion inducing lower blood flow than usual, which is one potential limitation of the current study.

Pixel-wise comparison yielded less-than-ideal results in this study despite the registration. This was partly ascribed to the distortion effects in the 2D EPI scan of DSC, especially noticeable in the object boundary (Figs. 2b, 3b). Also, relatively small number of subjects is another limitation of the current study. A different readout method for DSC may mitigate the distortion issue and testing in more subjects may show the true performance of the model. This study also showed perfusion maps from time-resolved CE-MRA that is not perfect, so further improvements need to be explored. The interval between the two injections of contrast agents was relatively short in this study. Acquiring T1 maps before second contrast injection was suggested to compensate for the variation in baseline T1 [28–30]. Baseline T1 map can be acquired using gradient echo with multiple flip angles followed by fitting process and this will help acquire even more accurate perfusion estimates [28]. According to our simulation, however, T1 varying from 1200 to 1800 ms (150-ms step) showed only 8.5% and 10% changes in CBV and Tmax, respectively (data not shown), which are relatively small and in agreement with other literature [28,29]. Also there are some reports that tumor grading with DCE MRI was not improved by using the independent T1 measurement compared to the fixed T1 assumption and thus usage of the fixed T1 may suffice for daily clinical practice [28–30].

In summary, the current study demonstrated the feasibility of mapping cerebral perfusion from time-resolved contrast enhanced MR angiographic data. The perfusion maps of CBV and Tmax from CE-MRA were visually and quantitatively correlated with those from DSC. Contrast enhanced MR angiography can provide not only topography of vascular structure but also the perfusion from the vasculature to surrounding tissue regions. This allows physician to receive both information in a single contrast agent injection, which reduces cost and improves patient safety and comfort.

Acknowledgements

This work was supported by the National Research Foundation of Korea (NRF-2017R1A2B2006526 and NRF-2018M3A9B5023527) and

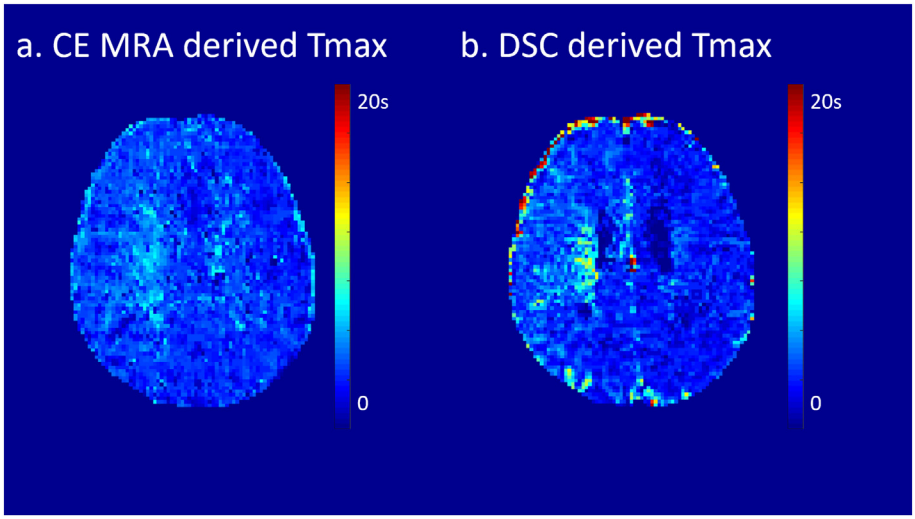

Fig. 3. Time-to-max (Tmax) maps from time-resolved contrast enhanced MR angiography (CE MRA) (a) and dynamic susceptibility contrast MRI (DSC) (b). Color scale bars represent the Tmax values.

Table 2
Correlation coefficients between perfusion maps (CBV, Tmax) from dynamic susceptibility contrast (DSC) MRI and time-resolved contrast enhanced MR angiography (CE-MRA). The values are described as mean ± standard deviation. SSIM: structural similarity, pixel-wise: pixel-wise correlation coefficients, ROI-based: ROI-based correlation coefficients, Gray Matter, White Matter, and Pathologic: ROI-based correlation coefficients in gray matter, white matter, and pathologic regions, respectively.

Parameters	Whole volume			Gray Matter (ROI-based)	White Matter (ROI-based)	Normal (ROI-based)	Pathologic (ROI-based)
	SSIM	Pixel-wise	ROI-based				
CBV	0.72 ± 0.08	0.45 ± 0.17	0.81 ± 0.10	0.82 ± 0.12	0.82 ± 0.09	0.87 ± 0.03	0.86 ± 0.03
Tmax	0.67 ± 0.05	0.22 ± 0.11	0.65 ± 0.11	0.70 ± 0.08	0.52 ± 0.33	0.49 ± 0.16	0.72 ± 0.41

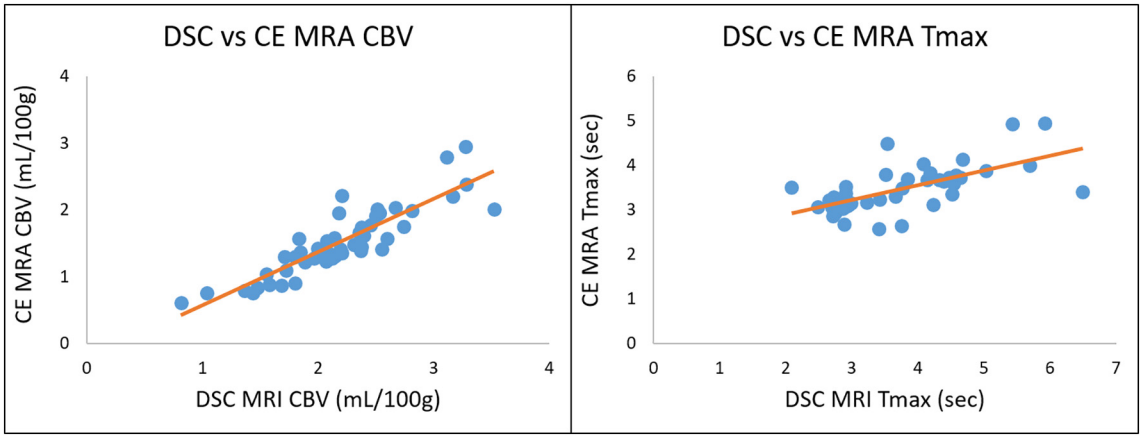

Fig. 4. ROI-based correlation plots between time-resolved contrast enhanced MR angiography (CE MRA) and dynamic susceptibility contrast MRI (DSC) for cerebral blood volume (CBV) (left) and time-to-maximum maps (Tmax) (right). The orange line indicates the trend line.

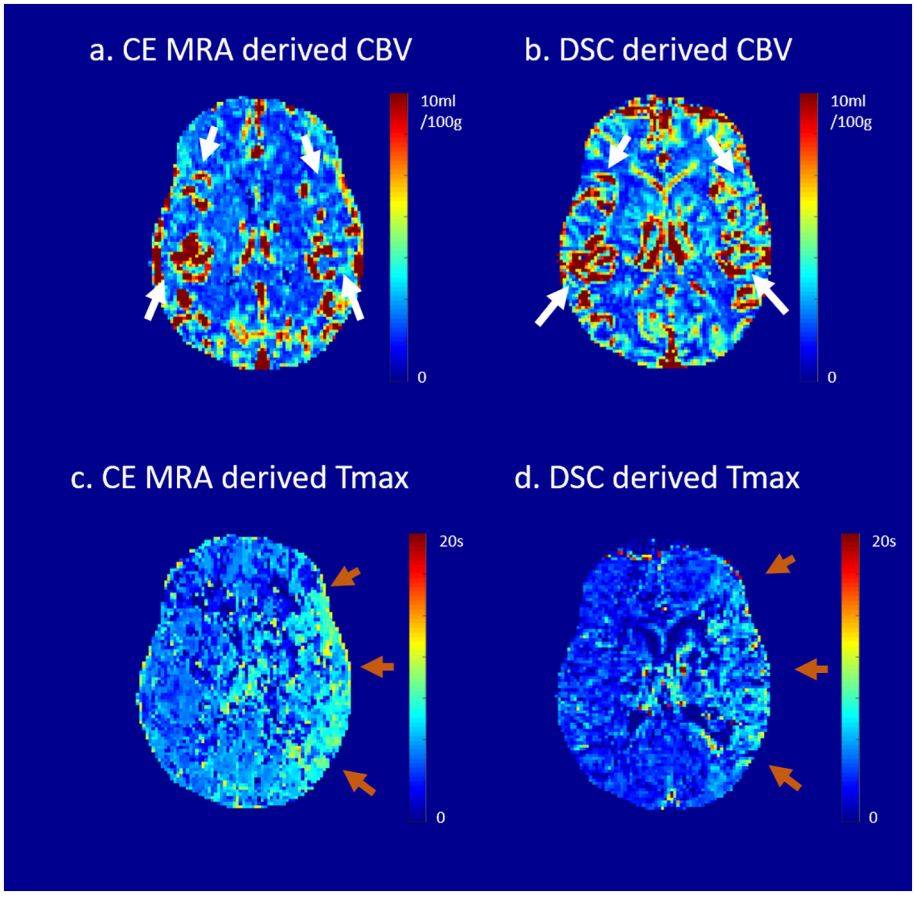

Fig. 5. Another representative cerebral blood volume (CBV) and time-to-max (Tmax) maps showing the occlusion site from a patient different from the one shown in Figs. 2 and 3. Left M1 occlusion site is indicated by brown arrows in Tmax maps. The area with Tmax > 6 s indicates the abnormal hemodynamic region that is clearly shown in Tmax maps from both methods (c,d). The CBV maps (a,b) also show clue for the hypo-perfusion as indicated by white arrows in comparison to the contralateral normal side. (For interpretation of the references to color in this figure legend, the reader is referred to the web version of this article.)

the Korea Health Technology R&D Project through the Korea Health Industry Development Institute (KHIDI), funded by the Ministry of Health & Welfare of South Korea (HI16C1111).

References

[1] Smith AM, Grandin CB, Duprez T, Mataigne F, Cosnard G. Whole brain quantitative CBF, CBV, and MTT measurements using MRI bolus tracking implementation and application to data acquired from hyperacute stroke patient. J Magn Reson Imaging 2000;12(3):400–10.

[2] Ostergaard L. Principles of cerebral perfusion imaging by bolus tracking. J Magn Reson Imaging 2005;22(6):710–7.

[3] Rezaie SR, Swaminathan A, Koyfman A, Long B. A new paradigm shift in acute ischemic stroke, large vessel occlusions, and endovascular therapy. J Emerg Med 2018;56(3):258–66.

[4] AJ Tsiouris, Qian Jenny, Kummer Benjamin R. Advanced imaging in acute ischemic stroke. Emerg Med Rep 2017;38.

[5] Haider CR, Hu HH, Campeau NG, Huston 3rd J, Riederer SJ. 3D high temporal and spatial resolution contrast-enhanced MR angiography of the whole brain. Magn Reson Med 2008;60(3):749–60.

[6] Zhang Y, Wang J, Wang X, Zhang J, Fang J, Jiang X. Feasibility study of exploring a T(1)-weighted dynamic contrast-enhanced MR approach for brain perfusion imaging. J Magn Reson Imaging 2012;35(6):1322–31.

[7] Uh J, Lewis-Amezcua K, Varghese R, Lu H. On the measurement of absolute cerebral blood volume (CBV) using vascular-space-occupancy (VASO) MRI. Magn Reson Med 2009;61(3):659–67.

[8] Perkio J, Aronen HJ, Kangasmaki A, Liu Y, Karonen J, Savolainen S, et al. Evaluation of four postprocessing methods for determination of cerebral blood volume and mean transit time by dynamic susceptibility contrast imaging. Magn Reson Med 2002;47(5):973–81.

[9] Carroll TJ, Horowitz S, Shin W, Mouannes J, Sawlani R, Ali S, et al. Quantification of cerebral perfusion using the "bookend technique": an evaluation in CNS tumors. Magn Reson Imaging 2008;26(10):1352–9.

[10] Shah MK, Shin W, Parikh VS, Ragin A, Mouannes J, Bernstein RA, et al. Quantitative cerebral MR perfusion imaging: preliminary results in stroke. J Magn Reson Imaging 2010;32(4):796–802.

[11] Marin-Padilla M. The human brain intracerebral microvascular system: development and structure. Front Neuroanat 2012;6:38.

[12] Olivot JM, Mlynash M, Zaharchuk G, Straka M, Bammer R, Schwartz N, et al. Perfusion MRI (Tmax and MTT) correlation with xenon CT cerebral blood flow in stroke patients. Neurology 2009;72(13):1140–5.

[13] Calamante F. Arterial input function in perfusion MRI: a comprehensive review. Prog Nucl Magn Reson Spectrosc 2013;74:1–32.

[14] Barnes SR, Ng TS, Montagne A, Law M, Zlokovic BV, Jacobs RE. Optimal acquisition and modeling parameters for accurate assessment of low Ktrans blood-brain barrier permeability using dynamic contrast-enhanced MRI. Magn Reson Med 2016;75(5):1967–77.

[15] Rohrer M, Bauer H, Mintorovich J, Requardt M, Weinmann HJ. Comparison of magnetic properties of MRI contrast media solutions at different field strength. Invest Radiol 2005;40(11):715–24.

[16] Chouhan MD, Bainbridge A, Atkinson D, Punwani S, Mookerjee RP, Lythgoe MF, et al. Estimation of contrast agent bolus arrival delays for improved reproducibility of liver DCE MRI. Phys Med Biol 2016;61(19):6905–18.

[17] Hamy V, Dikaios N, Punwani S, Melbourne A, Latifoltojar A, Makanyanga J, et al. Respiratory motion correction in dynamic MRI using robust data decomposition registration - application to DCE-MRI. Med Image Anal 2014;18(2):301–13.

[18] Mattes D, Haynor DR, Vesselle H, Lewellyn TK, Eubank W, Hanson KM. Nonrigid multimodality image registration. vol. 4322. 2001. p. 1609–20.

[19] Liu J, Wang Y, Akamatsu Y, Lee CC, Stetler RA, Lawton MT, et al. Vascular remodeling after ischemic stroke: mechanisms and therapeutic potentials. Prog Neurobiol 2014;115:138–56.

[20] Park CS, Payne SJ. Modelling the effects of cerebral microvasculature morphology on oxygen transport. Med Eng Phys 2016;38(1):41–7.

[21] Malinova V, Dolatowski K, Schramm P, Moerer O, Rohde V, Mielke D. Early whole-brain CT perfusion for detection of patients at risk for delayed cerebral ischemia after subarachnoid hemorrhage. J Neurosurg 2016;125(1):128–36.

[22] Koenig M, Klotz E, Luka B, Venderink DJ, Spittler JF, Heuser L. Perfusion CT of the brain: diagnostic approach for early detection of ischemic stroke. Radiology 1998;209(1):85–93.

[23] Zakariaee SS, Oghabian MA, Firouznia K, Sharifi G, Arbabi F, Samiei F. Assessment of the agreement between cerebral hemodynamic indices quantified using dynamic susceptibility contrast and dynamic contrast-enhanced perfusion magnetic resonance Imagings. J Clin Imaging Sci 2018;8:2.

[24] Zakhari N, Taccone MS, Torres CH, Chakraborty S, Sinclair J, Woulfe J, et al. Prospective comparative diagnostic accuracy evaluation of dynamic contrast-enhanced (DCE) vs. dynamic susceptibility contrast (DSC) MR perfusion in differentiating tumor recurrence from radiation necrosis in treated high-grade gliomas. J Magn Reson Imaging 2019. (in press).

[25] Tan JC, Dillon WP, Liu S, Adler F, Smith WS, Wintermark M. Systematic comparison of perfusion-CT and CT-angiography in acute stroke patients. Ann Neurol 2007;61(6):533–43.

[26] Chen F, Ni YC. Magnetic resonance diffusion-perfusion mismatch in acute ischemic stroke: an update. World J Radiol 2012;4(3):63–74.

[27] Takasawa M, Jones PS, Guadagno JV, Christensen S, Fryer TD, Harding S, et al. How reliable is perfusion MR in acute stroke? Validation and determination of the penumbra threshold against quantitative PET. Stroke 2008;39(3):870–7.

[28] Haacke EM, Filleti CL, Gattu R, Ciulla C, Al-Bashir A, Suryanarayanan K, et al. New algorithm for quantifying vascular changes in dynamic contrast-enhanced MRI independent of absolute T1 values. Magn Reson Med 2007;58(3):463–72.

[29] Tietze A, Mouridsen K, Mikkelsen IK. The impact of reliable prebolus T 1 measurements or a fixed T 1 value in the assessment of glioma patients with dynamic contrast enhancing MRI. Neuroradiology 2015;57(6):561–72.

[30] Jung SC, Yeom JA, Kim JH, Ryoo I, Kim SC, Shin H, et al. Glioma: application of histogram analysis of pharmacokinetic parameters from T1-weighted dynamic contrast-enhanced MR imaging to tumor grading. AJNR Am J Neuroradiol 2014;35(6):1103–10.